

# A Quantum Chemical Study of the Mechanism of Tyrosinase

Torulf Lind and Per E. M. Siegbahn\*

Department of Physics, Stockholm University, Box 6730, S-113 85 Stockholm, Sweden

Robert H. Crabtree

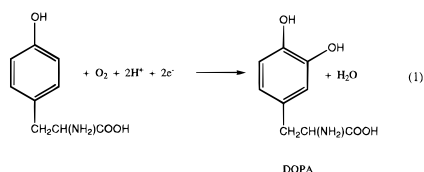
Chemistry Department, Yale University, 225 Prospect Street, New Haven, Connecticut, 06520-8107

Received: May 20, 1998; In Final Form: October 28, 1998

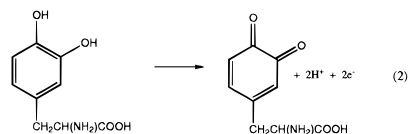
Density functional calculations (DFT-B3LYP) on a neutral model system  $L_3Cu\cdots CuL_3$  have been carried out to probe the mechanism of tyrosinase action. The ligands L are chosen either as ammonia or formimine to model the real histidine ligands. Most of the effort of the project was put into locating the transition state for O–O activation of  $O_2$  for both sets of ligands. It is found that the activation occurs on the antiferromagnetically coupled singlet surface, here modeled as a triplet. This is the ground state of the initially formed peroxide complex. The activation leads to an excited bis- $\mu$ -oxo state which is converted exothermically to the closed shell singlet product after the reaction. The peroxide complex is found to have a nonplanar Cu–O<sub>2</sub>–Cu arrangement, while the Cu–O<sub>2</sub>–Cu ring in the bis- $\mu$ -oxo product is planar. The barrier for  $O_2$  activation found for the formimine case is 15.1 kcal/mol and for the ammonia case is 13.6 kcal/mol, both in line with the overall experimental reaction rate for the entire tyrosinase cycle of  $10^3\text{ s}^{-1}$ , indicating that  $O_2$  activation is rate limiting. As an initial attempt toward modeling the subsequent steps of the phenol oxidation, only the computationally simplest approach was tried, which involves transient radical intermediates. The computed energetics suggest that this route might be feasible even though one step may be slightly too endothermic. The relevance of the findings to the enzyme and the limitations of the model are also discussed.

## I. Introduction

Tyrosinase (Ty), perhaps the best known dicopper oxygenase,<sup>1,2</sup> carries out the aerobic oxidation of phenols to *o*-diphenols (cresolase reaction, eq 1) and the subsequent con-



version of the *o*-diphenol to the *o*-quinone (catecholase reaction, eq 2) in bacteria, plants, and animals. Of these, eq 1 is



intrinsically the slower step and therefore normally turnover limiting. With tyrosine itself as the substrate, the intermediate oxidation product is DOPA, the quinone of which spontaneously polymerizes to form the pigment, melanin. As a monooxygenase, tyrosinase requires a  $2e^-$  reducing agent to carry out eq 1, a step in which the second O of dioxygen is reduced to water. These two electrons come from the second, catecholase step of the reaction (eq 2).

Although no crystal structure is available for tyrosinase itself, the structures of both the deoxy and oxy forms of the very

closely related mollusc and arthropod dioxygen transport protein, hemocyanin (Hc), are available,<sup>3,4</sup> see Figure 1 and 2. In deoxy-Hc, each Cu(I) is three-coordinate with a pyramidal geometry and a long Cu $\cdots$ Cu distance (3.16 Å) appropriate for a weak metal–metal interaction. In oxy-Hc, each Cu(II) is 5-coordinate with a distorted geometry that is perhaps best described as square pyramidal, with the axial Cu–N(His) distances being quite long (2.4–2.5 Å). The  $\mu$ - $\eta^2$ - $\eta^2$  peroxide binding is a striking and unusual feature of the system. Sequence analogies and chemical and spectroscopic studies suggest a very close relationship between the Hc and Ty active sites, except that Hc is not capable of reaction with phenolic substrates, partly as a result of Hc having an extra domain that blocks access to the active site.<sup>1,2</sup> It is now clear both from sequence homologies and spectroscopic data that the active site of Ty also has a (His)<sub>3</sub> Cu $\cdots$ Cu(His)<sub>3</sub> arrangement with a geometry rather similar to that in Hc and that it binds  $O_2$  in the same way as does Hc.<sup>4,1</sup>

Several different states of tyrosinase have been detected. The Cu(I)Cu(I) deoxy form reacts with  $O_2$  to give the Cu(II)Cu(II) oxy form. Resonance Raman data on isotopically labeled samples indicated a symmetric peroxide coordination mode with a very low  $\nu$  (O–O) of ca.  $750\text{ cm}^{-1}$ , now recognized to be the very unusual  $\mu$ - $\eta^2$ - $\eta^2$  peroxide structure shown in Figure 2.<sup>6</sup>

Deoxy-Ty can also be one electron oxidized in the absence of  $O_2$  but the presence of a variety of exogenous ligands such as azide or nitrite gives the half-met Cu(I)Cu(II) form. Further oxidation can give Cu(II)Cu(II) forms, either in EPR-detectable or in EPR, nondetectable forms; the difference is believed to reside in the Cu–Cu distance, short (ca. 3.4 Å) with a bridging

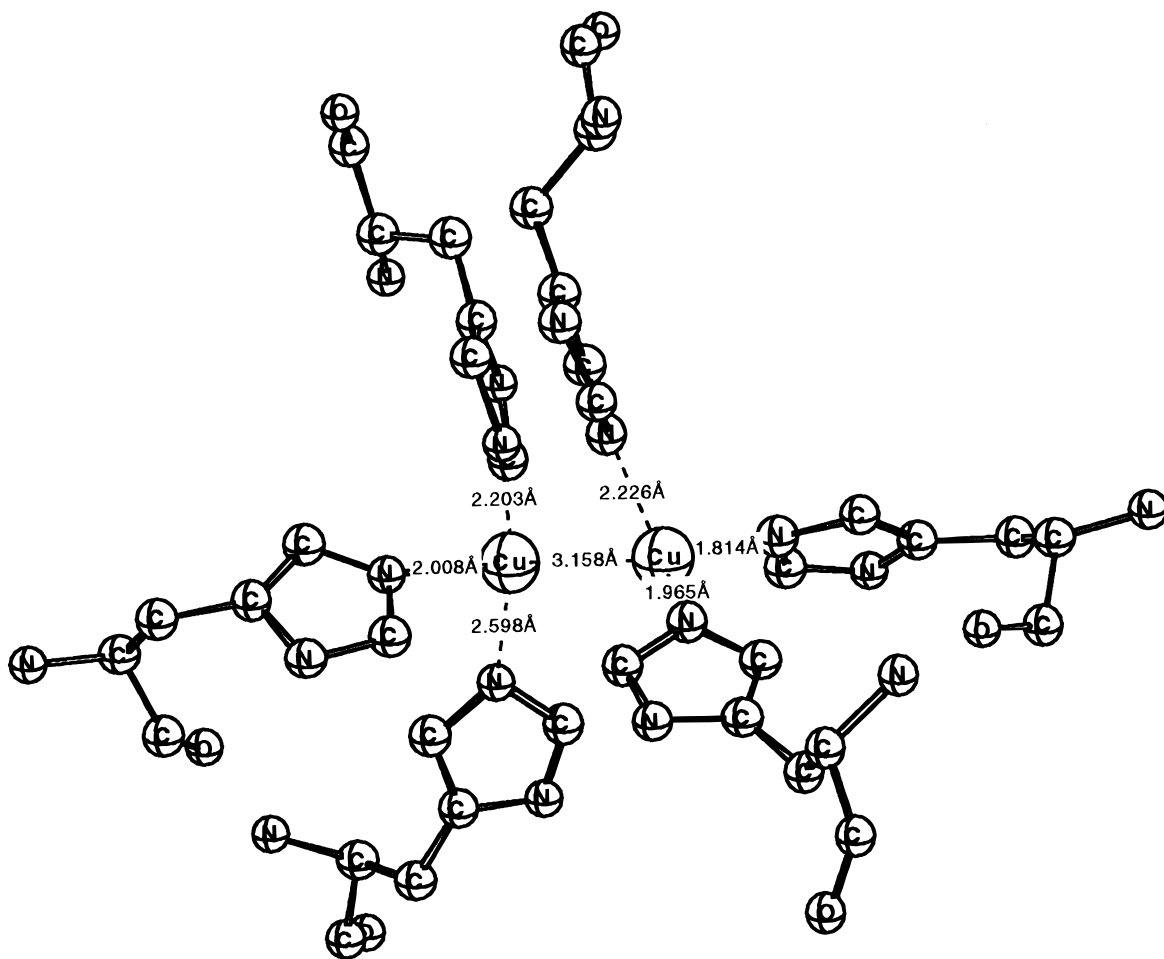
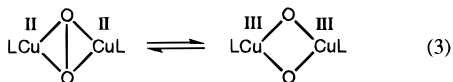


**Figure 1.** X-ray structure of the deoxy form of hemocyanin.

ligand (probably  $\text{OH}^-$ )<sup>3</sup> to provide electronic coupling for the nondetectable, and long (ca. 6 Å) for the EPR-detectable forms.

Important contributions have been made in the area of model compounds. A planar  $\mu\text{-}\eta^2\text{-}\eta^2$  peroxide  $\text{Cu(II)Cu(II)}$  dimer of the type  $[\text{TpCu}(\text{O}_2)\text{CuTp}]$  ( $\text{Tp} = \text{HB}3,5\text{-iPr}_2\text{-pyrazolyl}$ ) was isolated by Kitajima et al.<sup>6,7</sup> as a model of oxy-Hc. Karlin<sup>8</sup> showed how a di-copper(I) model containing a meta-xylyl bridging group was hydroxylated at the arene CH bond on reaction with  $\text{O}_2$ , thus modeling the CH activation step of tyrosinase. An attack of an electrophilic oxygen of an intermediate  $\mu\text{-}\eta^2\text{-}\eta^2$  peroxide on the arene ring is strongly indicated by the experimental evidence on the model system. Mechanisms not involving hydroxylation but implicating direct conversion of the tyrosine to the quinone have also been proposed.<sup>8,6</sup> Remarkably, Tolman and co-workers<sup>10</sup> find that a  $\mu\text{-}\eta^2\text{-}\eta^2$  peroxide  $\text{Cu(II)Cu(II)}$  dimer can be reversibly converted by O–O bond cleavage to a bis- $\mu\text{-oxo-Cu(III)Cu(III)}$  dimer (eq 3, L = triazacyclononane) under very mild conditions; no such



species has been observed in Hc or Ty, however.

Solomon and co-workers<sup>11</sup> have suggested that the phenol binds to one copper and the arene ring undergoes electrophilic attack by one of the bridging O atoms. It was not possible to say whether O–O bond cleavage precedes, accompanies, or follows phenol coordination. A recent review of the mechanism is available.<sup>11b</sup> Two model studies on the binding of  $\text{O}_2$  to a

copper dimer in the peroxide state have recently been published.<sup>12,13</sup> CASSCF, CASPT2, and DFT calculations with gradient corrections but without Hartree–Fock exchange were performed. Using a restricted geometry optimization at the DFT level and with ammonia as model ligands and a doubly charged complex, the singlet state was found to be preferred by 13.3 kcal/mol compared to the triplet state. In a single-point calculation using imidazole ligands, this splitting increased to 26.9 kcal/mol, which can be compared to the experimental splitting found to be greater than 1.7 kcal/mol.<sup>11</sup> In the present model calculations discussed below performed for a neutral model, the singlet is preferred in agreement with experiment and the computed splitting is 1.0 kcal/mol using ammonia ligands. The CASPT2 calculations in ref 12 were only performed for a model without ligands where the triplet was found to be the preferred ground state by 44.4 kcal/mol. For the same model system, the DFT calculations also gave a preferred triplet state but only by 3.8 kcal/mol. In the present paper, we look at quantum chemical models of the active site structure to test some of the proposals that have been made.

## II. Computational Details

The calculations were performed in two steps. First, an optimization of the geometry was performed using the B3LYP method<sup>14</sup> with double- $\zeta$  basis sets. In the second step, the energy was evaluated for the optimized geometry using very large basis sets including diffuse functions and with two polarization functions on each atom. The final energy evaluation was also performed at the B3LYP level. All calculations were made using the GAUSSIAN-94 program.<sup>15</sup>

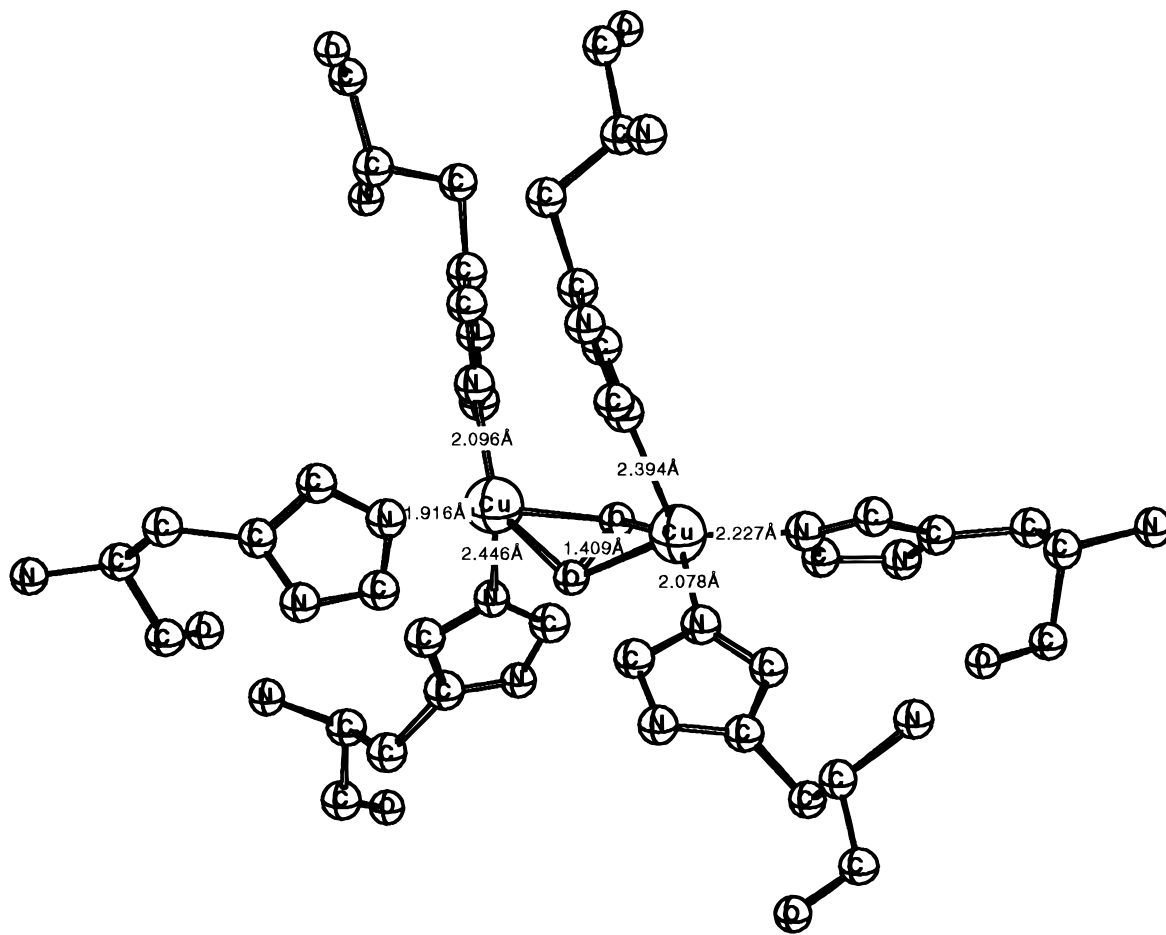


**Figure 2.** X-ray structure of the peroxide form of hemocyanin.

The B3LYP functional can be written as<sup>14,16</sup>

$$F^{\text{B3LYP}} = (1 - A)F_x^{\text{Slater}} + AF_x^{\text{HF}} + BF_x^{\text{Becke}} + CF_c^{\text{LYP}} + (1 - C)F_c^{\text{VWN}}$$

where  $F_x^{\text{Slater}}$  is the Slater exchange,  $F_x^{\text{HF}}$  is the Hartree–Fock exchange,  $F_x^{\text{Becke}}$  is the gradient part of the exchange functional of Becke,<sup>14</sup>  $F_c^{\text{LYP}}$  is the correlation functional of Lee, Yang, and Parr,<sup>17</sup> and  $F_c^{\text{VWN}}$  is the correlation functional of Vosko, Wilk, and Nusair.<sup>18</sup>  $A$ ,  $B$ , and  $C$  are the coefficients determined by Becke<sup>14</sup> using a fit to experimental heats of formation, but Becke did not use  $F_c^{\text{VWN}}$  and  $F_c^{\text{LYP}}$  in the expression above when the coefficients were determined, but used the correlation functionals of Perdew and Wang instead.<sup>18</sup>

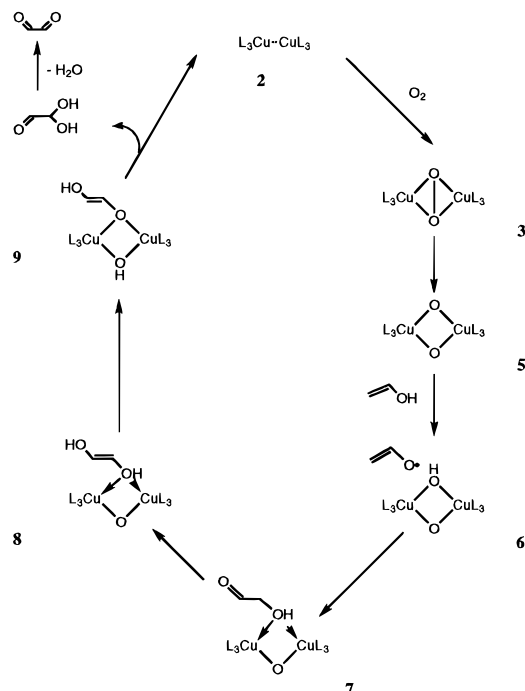
The B3LYP energy calculations were for all the copper dimer models made using the large 6-311+G(2d,2p) basis sets in the GAUSSIAN-94 program. This basis set has two sets of polarization functions on all atoms, including two f-sets on the metals, and also diffuse functions. In the B3LYP geometry optimizations, a much smaller basis set, the LANL2DZ set of the Gaussian-94 program, was used in most cases. For the copper atoms this means that a nonrelativistic ECP according to Hay and Wadt<sup>20</sup> was used. The metal valence basis set used in connection with this ECP is essentially of double- $\zeta$  quality. The rest of the atoms are described by standard double- $\zeta$  basis sets. A few exceptions to this general recipe for performing the calculations were made. First, in a few geometry optimizations the effects of d-functions on nitrogen were tested. Second, for the largest systems studied here containing the six actual histidine ligands, no additional large basis set calculation could

be afforded so the energies discussed below are for the same basis set as was used for the geometry optimization. Whenever there has been a deviation from the general procedure for doing the calculations, this will be explicitly mentioned in the text below.

The calculation of Hessians and thereby the zero-point vibrational effects are quite expensive for the present systems. Since these effects are not large or critical for the qualitative conclusions drawn in this study, these effects were obtained at the Hartree–Fock level. The effects were scaled by a factor of 0.9 as usual. All energies discussed below contain these effects.

### III. Results and Discussion

A large part of every quantum chemical study of an enzymatic reaction has to be concerned with the model used for the enzyme. Knowledge of the X-ray structure of the protein is normally necessary for setting up reasonable models to study the reaction mechanisms of the enzyme. In the present case of tyrosinase, such structures are available for the closely related hemocyanin enzyme, see Figures 1 and 2, and these structures are used for choosing the present model. Even when a structure is known, there are normally two other problems that need to be carefully investigated before the enzyme reaction can be studied. First, the most likely oxidation states have to be determined in some way. In two recent studies on hydrogenase<sup>21</sup> and nitrogenase,<sup>22</sup> this took up a large part of the initial effort devoted to the projects. In the present case, the oxidation states of the active state of the enzyme are known with near-certainty, which simplifies the present study considerably. The starting deoxy form of the dimer, before oxygen is added, has oxidation

**SCHEME 1: Pathway Investigated for Tyrosinase with the Model Substrate, Vinyl Alcohol**


states of Cu(I)–Cu(I). The preliminary model investigations could therefore be restricted to the second major question, namely, the choice of model ligands. This choice has to be in reasonable accord with the actual ligands in the complex, but the ligands should be as small as possible to allow efficient computation. Choosing the ligands of the X-ray structure, in this case six histidines, would make the model calculations cumbersome and so severely limit our ability to make the numerous tests of the reaction mechanisms that are usually required. On the other hand, if simple ligands are used, the limitations of these ligands have to be investigated in order to interpret the results properly. The tyrosinase reaction sequence followed in this study is shown in Scheme 1. The most critical, and also most interesting, part of this sequence occurs in the initial steps. First, the binding in the reactant  $L_3-Cu-Cu-L_3$  deoxy dimer turns out to be more difficult to describe than expected. Second, the binding of  $O_2$  between the copper atoms and the step where the O–O distance is increased going from the peroxide form to the bis- $\mu$ -oxo form is where different mechanisms have been suggested. These steps are therefore the ones where most effort of the present project was placed. The problems describing the reactant dimer had to be overcome by trying different ligand models. For the  $O_2$  forms of tyrosinase different spin states were tried and a transition state for breaking the O–O bond was also located. The steps investigated following the  $O_2$  activation should only be regarded as a very preliminary investigation of a possible reaction sequence. A radical sequence was chosen as the first of several possible pathways simply because it is the easiest one to treat computationally. The more plausible electrophilic pathway will be investigated in a future study.

**a. Chemical Model.** The copper atoms of the tyrosinase enzyme are both three-coordinate with histidine ligands and the oxidation states of the deoxy form is Cu(I)–Cu(I). There are essentially two different ways to model these oxidation states in the computations. One could choose neutral ligands in which case the charge of the entire complex would be +2. This was the model used in a recent theoretical study of a complex closely

**TABLE 1: Relative Energies (kcal/mol) for the First Part of the Tyrosinase Reaction Sequence Using Formimine Ligands (L). Numbering of the Intermediates Refer to Scheme 1**

structure	intermediate		
	state	no.	energy
$2 \times L_3 Cu$ (monomer)	$^1A$	<b>1</b>	0.0
$L_3Cu-CuL_3$ (dimer)	$^1A$	<b>2</b>	-22.5
$L_3Cu-O_2-CuL_3$ (peroxide)	$^1A$	<b>3</b>	-14.9
$L_3Cu-O_2-CuL_3$ (peroxide)	$^3A$	<b>3</b>	-23.2
$O_2$ activation transition state	$^3A$	<b>4</b>	-8.1
$L_3Cu-O-O-CuL_3$ (bis- $\mu$ -oxo)	$^1A$	<b>5</b>	-38.6
$L_3Cu-O-O-CuL_3$ (bis- $\mu$ -oxo)	$^3A$	<b>5</b>	-17.2

**TABLE 2: Relative Energies (kcal/mol) for the Tyrosinase Reaction Sequence Using Ammonia Ligands (L). Numbering of the Intermediates refer to Scheme 1**

structure	intermediate		
	state	no.	energy
$2 \times L_3Cu$ (monomer)	$^1A$	<b>1</b>	0.0
$L_3Cu-CuL_3$ (dimer)	$^1A$	<b>2</b>	-23.2
$L_3Cu-O_2-CuL_3$ (peroxide)	$^1A$	<b>3</b>	-2.0
$L_3Cu-O_2-CuL_3$ (peroxide)	$^3A$	<b>3</b>	-10.1
$O_2$ activation transition state	$^3A$	<b>4</b>	3.5
$L_3Cu-O-O-CuL_3$ (bis- $\mu$ -oxo)	$^1A$	<b>5</b>	-30.7
$L_3Cu-O-O-CuL_3$ (bis- $\mu$ -oxo)	$^3A$	<b>5</b>	-8.7
$L_3Cu-OH-O-CuL_3 + C_2H_3O^*$	$^2A$	<b>6</b>	-30.6
$L_3Cu-O-CH_2(OH)CHO-CuL_3$	$^1A$	<b>7</b>	-58.1
$L_3Cu-O-C_2H_2(OH)_2-CuL_3$	$^1A$	<b>8</b>	-50.9
$L_3Cu-OH-CH(OH)CHO-CuL_3$	$^1A$	<b>9</b>	-55.6
$L_3Cu-CuL_3$ (dimer) + $C_2O_2H_2 + H_2O$	$^1A$	<b>10</b>	-92.6

related to tyrosinase.<sup>23</sup> With this type of model, it is normally assumed that the positive charge is predominantly located on the ligands and stabilized by anionic second sphere ligands. This choice may require the second sphere ligands to be included in the model for realistic interaction energies to be obtained. In the previous theoretical study, which did not include second sphere ligands, the charged form of the oxidized complex was found to be unstable to dissociation into fragments. This problem was dealt with by going to a lower level geometry optimization (SCF level) at which the system held together and where a quite reasonable geometry was obtained. However, this type of approach is clearly rather dangerous, since it is found (in the present study) that the doubly charged peroxide complex is unstable with respect to dissociation into fragments by as much as 60 kcal/mol using ammonia ligands. In the present study, a different type of modeling the oxidation states is therefore used. From previous model studies it has been shown that it is often more satisfactory to model enzyme complexes as neutral species. The idea is that the tendency for charge accumulation should be small in the low dielectric medium of a protein where the dielectric constant is about 4. To get the proper Cu(I)–Cu(I) oxidation states, one of the ligands on each copper atom is therefore chosen anionic. In the present studies, the histidine ligands were initially replaced by ammonia ligands and later on by formimine ligands ( $CH_2=NH$ ). The formimine ligand models have the advantage that metal-to-ligand  $\pi$ -bonding is present and they should also be somewhat less apt to form unwanted hydrogen bonds since there is only one N–H bond present. With these major modeling aspects, the model for the deoxy form of tyrosinase with ammonia ligands becomes  $(H_3N)_2(H_2N)-Cu\cdots Cu-(NH_2)(NH_3)_2$ . With the lack of total charge of this complex the problem of dissociation into fragments should not be present. The resulting energies using formimine ligands are given in Table 1 and those with ammonia ligands in Table 2.

**b. Monomer and Dimer Reactants.** The first structure investigated in detail was the reactant  $L_3-Cu-Cu-L_3$ . X-ray

structures of several complexes of this type exist;<sup>3</sup> see, for example, Figure 1. A notable feature in these structures is that the Cu–Cu distance varies significantly from structure to structure and that this distance is often quite long, in the range 2.9–3.6 Å. These structural results indicate a rather weak binding between the monomers. This is expected since any metal–metal binding would require a costly Cu(I) to Cu(II) promotion. The first structure optimization of the dimer using ammonia ligands gave a Cu–Cu distance of 3.13 Å, well in line with the experimental distances. However, the binding energy with respect to two monomers is as large as 23.2 kcal/mol, which is a quite surprising value. From the structure obtained it is clear that the origin of this binding probably in large part comes from strong hydrogen bonding between ligands on different copper centers. In particular, there are two interactions of type Cu–NH<sub>2</sub>···H<sub>3</sub>–Cu that are quite strong. This type of interaction cannot be present in the real enzyme where there are only histidines, so this part of the binding energy must be an artifact. To investigate this problem further, an optimization was performed using formimine ligands for which it might be possible to avoid the artificial hydrogen bonding. However, starting the geometry optimization from the experimental structure without hydrogen bonding, the structure soon reorganizes to form the same hydrogen bonds as when ammonia ligands were used. The binding energy between the monomers is only 0.7 kcal/mol smaller with the formimine ligands than with the ammonia ligands. To get a realistic estimate of the true interaction, it therefore appears that using six imidazole ligands must be used even though this is quite expensive. The outcome of this geometry optimization was very clear: the monomers departed from each other indicating a zero or very small binding energy of the dimer. The simplest possible procedure for accounting for the artifact of the binding energy of the dimer is therefore simply to set this energy to zero. This means that all energies will be counted from the monomers rather than from the dimer and this is what has been done in the tables and in the figures.

A second minor artifact, probably of small consequence for the energetics, also occurred for the monomer and dimer reactants with ammonia ligands. In the monomer Cu(I) complex one Cu–NH<sub>3</sub> became quite long, 3.10 Å, and in the dimer one distance for each copper became very long, 3.76 and 3.91 Å, compared to the longest Cu–N distance for the experimental structure in Figure of 2.60 Å. In this case, a combination of the lack of  $\pi$ -bonding to the metal and the presence of too strong hydrogen bonding between ammonia ligands is the main origin of this artifact. Changing to a ligand set based on formimine, which can give some metal  $\pi$ -bonding, corrects the problem. The longest Cu–N distance for the monomer with formimine ligands is 2.21 Å and for the dimer it is 2.16 Å. If imidazole ligands are used, the longest Cu–N distance is 2.06 Å for the monomer and 2.11 Å for the dimer. Since this effect is only an indirect electronic effect on the tyrosinase reaction energies, the direct effect on the reaction energies of having ammonia ligands should still be quite small.

**c. Peroxide and Bis- $\mu$ -oxo Complexes.** Probably the most interesting part of the tyrosinase reaction sequence occurs when O<sub>2</sub> is added and when the O–O bond is broken. In the first step, O<sub>2</sub> is placed between the copper atoms in a peroxide structure keeping the O–O bond. Two possible spin states are of interest. First, since the reactant dimer is a singlet and O<sub>2</sub> a triplet, a loosely coupled complex between the reactants should be a triplet. Second, if the Cu–O interaction increases, a singlet state may also be possible. Model calculations were performed

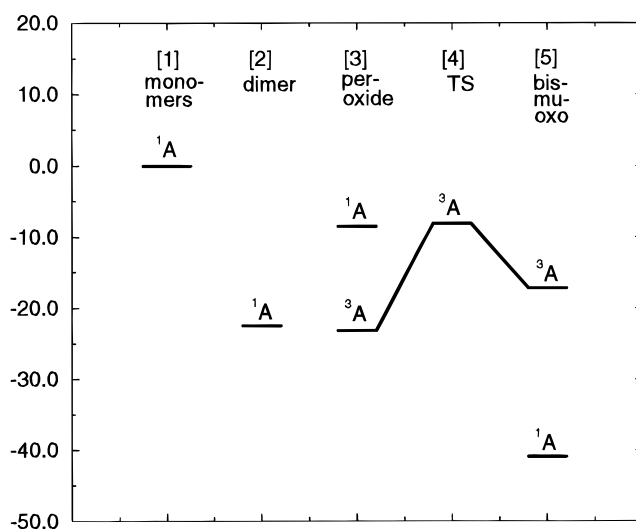


**Figure 3.** Energy diagram for the first part of the reaction sequence using formimine ligands.

both with ammonia and formimine ligands, but the details of the structures will only be discussed here for the case with formimine ligands. When the structures with ammonia ligands differ significantly, these differences will be pointed out. The energy diagram for the first part of the reaction sequence using formimine ligands is given in Figure 3.

There are a few characteristic features of the optimized triplet peroxide structure in Figure 4. First, one copper has one quite long Cu–N distance of 3.56 Å. This feature is present to some extent also in the X-ray structure with Cu–N distances of 2.39 and 2.45 Å, see Figure 2, and is due to strong Jahn–Teller (JT) distortions. This is expected for a Cu(II)–Cu(II) dimer. Strong cases of JT distortions have also recently been found computationally for another important metal dimer complex, compound **Q** of methane monooxygenase (MMO).<sup>26</sup> In that case the JT distortions play a significant role in the methane activation process, by allowing the bis- $\mu$ -oxo diamond core structure to open up and abstract a hydrogen. In the copper dimer case the JT distortions do not play quite such a direct mechanistic role, but they are still significant for the energetics of the reactions. Attempts were made to find an alternate minimum of the peroxide structure without any such long Cu–N distance as 3.56 Å but without success. Instead other structures were found with very similar energies where two Cu–N distances are long. These minima correspond to different hydrogen bonding situations. As seen in Figure 4, the formimine ligand with the long Cu–N distance has a hydrogen bond to one of the oxygens of the peroxide ligand. A second important feature of the triplet peroxide structure is that all four Cu–O distances are rather equal. The optimized Cu–O distances are 1.94, 1.97, 2.01, and 2.07 Å and the experimental values are 1.92, 2.08, 2.10, and 2.23 Å. This is rather surprising since each oxygen only has one covalent bond to copper. The other bond should be of lone-pair donor type and is normally expected to be weaker and longer. The Cu–O distances in the peroxide instead indicate strong delocalization of the covalent character into all four Cu–O bonds. Another interesting feature is the rather pronounced bending of the complex at the peroxide bridge. This bending is quite exaggerated in the optimized structure with a Cu–O<sub>2</sub> (midpoint)–Cu angle of only 116°, but is present also in the experimental structure with an angle of 152°. Since there is such a large discrepancy between the calculated and experimental angle, it appears that this is a quite sensitive property of the complex without much influence on the energy. The

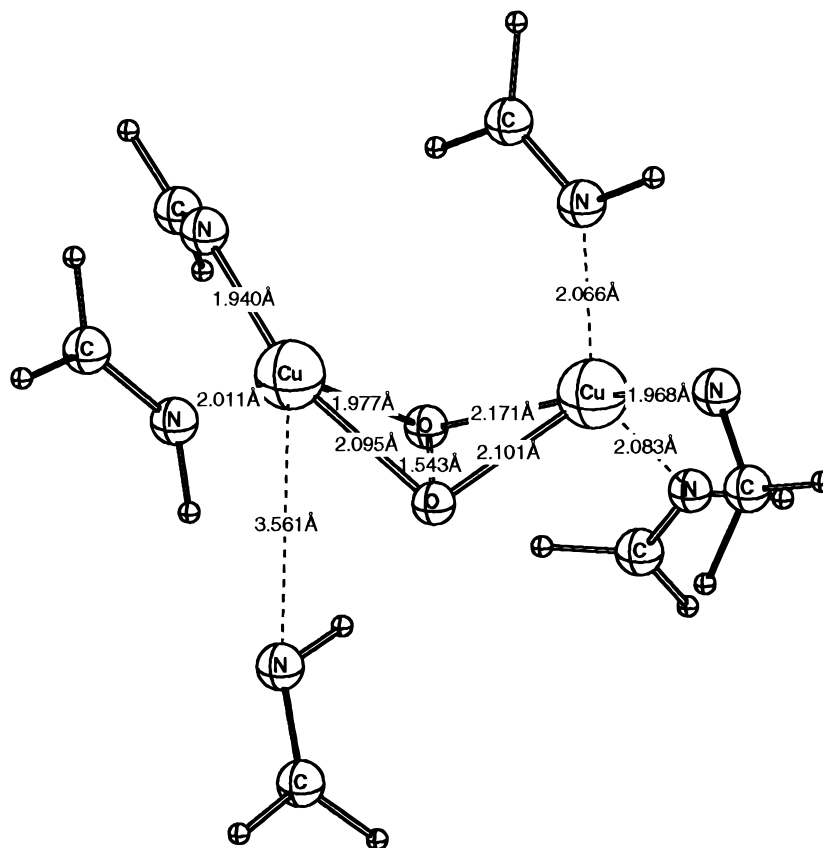


**Figure 4.** Optimized geometry for the triplet peroxide structure.

optimized O—O bond distance is 1.54 Å compared to the experimental value of 1.41 Å and of 1.21 Å for the isolated O<sub>2</sub>, indicating significant O<sub>2</sub> activation. This long O—O distance is also consistent both with the very low O—O stretching frequency of 755 cm<sup>-1</sup> found in the resonance Raman spectrum for oxy-Hc and oxy-Ty, and with the ready cleavage of the O—O bond in the next step. The spins on copper are 0.49 and 0.53 showing that as much as 0.98e is delocalized over the ligands. Some of this spin is on the oxygens which have spin populations of 0.21 and 0.16. The binding energy of the oxygen molecule in the peroxide complex is found to be 23.2 kcal/mol. As described above, this binding energy is counted from the two separated monomers since the dimer reactant is unbound. Because the binding energy of O<sub>2</sub> is as large as 23.2 kcal/mol and the monomers do not bind before the addition of O<sub>2</sub>, a barrier for the O<sub>2</sub> addition step on the triplet surface is unlikely. No attempt was therefore made to locate a transition state which would have required the use of the costly imidazole ligands.

The second possible state for the peroxide structure is a singlet. The structure obtained for the closed shell singlet state is in many ways similar to the one in Figure 4 for the triplet including a very similar O—O distance of 1.53 Å. However, an important difference is that the copper and oxygen atoms are now in one plane. The binding energy of O<sub>2</sub> for this structure is only 8.4 kcal/mol, significantly less than the 23.2 kcal/mol obtained for the triplet state.

The copper spins in the peroxide triplet state were ferromagnetically coupled in order to simplify the calculations. It has been a general experience, for example, for manganese<sup>27</sup> and iron dimers,<sup>26</sup> that ferromagnetic and antiferromagnetic coupling between the metal spins give very similar energies, with the antiferromagnetic coupling normally slightly preferred. This is true also for the copper dimer peroxide which is known to be EPR silent.<sup>1</sup> To test if the energy difference between the metal

spin-couplings is small also for the present systems, the antiferromagnetically coupled singlet state was also optimized. It turns out that both the energy and geometry are very similar to the ones for the ferromagnetically coupled triplet state. The energy splitting is only 0.4 kcal/mol for the formimine ligands and 1.0 kcal/mol for the ammonia ligands, both in favor of the antiferromagnetic coupling. Magnetic susceptibility measurements show that the antiferromagnetic singlet is more than 600 cm<sup>-1</sup> (1.7 kcal/mol) lower than the ferromagnetic triplet state.<sup>11</sup> Since the experimental result is just a lower bound, it is difficult to draw a firm conclusion concerning the agreement between the present results and experiment. However, the results from the previous theoretical study by Bernardi et al.<sup>12,13</sup> differs substantially from the present one concerning the size of the splitting. In the previous study a splitting of 13.3 kcal/mol was obtained for the case with ammonia ligands, and the splitting increased to 26.9 kcal/mol in a single-point calculation using imidazole ligands. The major difference to our results is due to the use of a doubly charged model complex in refs 12 and 13. As noted above, a doubly charged model complex with ammonia ligands is unstable with respect to dissociation into fragments by 60 kcal/mol at the B3LYP level. For imidazole ligands the charged complex is unstable by about 30 kcal/mol. This instability leads to a quite different type of bonding for the charged complex involving a large contribution of electrostatic bonding to a singlet O<sub>2</sub> molecule. The use of different functionals and geometries may also contribute to the difference of the results. It is emphasized in refs 12 and 13 that for large systems it is better to use a model where key parameters of the geometries are fixed at the experimental values. Even though there may be cases where this turns out to be the case, it is at least not always true. It has been shown for blue copper proteins, for example, that excellent geometries in comparison to experiments can be obtained by full geometry optimizations of metal

complexes in proteins.<sup>28</sup> Going back to the present results, the copper–ligand distances differ by less than 0.03 Å between the two coupling cases. The spin distribution in the two coupling cases differ somewhat. With ferromagnetic coupling the spins on copper are 0.49 and 0.53, while with antiferromagnetic coupling they are –0.38 and 0.39.

When the O–O bond of O<sub>2</sub> is broken a bis- $\mu$ -oxo Cu(III)–Cu(III) structure is obtained. This intermediate has not been detected in the enzyme but is seen in model compounds. The ground state for this structure is a closed shell singlet as appropriate for Cu(III), unlike the singlet form of the peroxide structure which is an antiferromagnetically coupled singlet state. The copper and oxygen atoms are all in one plane in the singlet bis- $\mu$ -oxo structure, which is different from the case of the triplet peroxide structure where there was a significant bending at the oxygens. The binding energy of O<sub>2</sub> is also substantially stronger with 38.6 kcal/mol for the bis- $\mu$ -oxo structure compared to 23.2 kcal/mol for the peroxide structure. The formimine ligand positions are very similar in the triplet peroxide and the singlet bis- $\mu$ -oxo structures, still with one very long Cu–N distance of 3.65 Å due to hydrogen bonding to an oxygen. As expected for a normal bis- $\mu$ -oxo structure, the Cu–O distances are all quite similar with values of 1.83, 1.88, 1.91, and 1.91. In contrast, for compound Q of MMO, which was severely JT distorted, the metal–oxygen distances were found to be substantially different with two short distances of 1.7 Å and two long distances of 2.0 Å. These differences between the bis- $\mu$ -oxo structures indicate that the O<sub>2</sub> activation mechanism could also be quite different for the two systems.

The second spin-coupling possibility for the bis- $\mu$ -oxo structure is a triplet state. As before, the antiferromagnetically coupled singlet state should be very close in energy and only the triplet state was therefore optimized. It was found to be bound by 17.2 kcal/mol with respect to the reacting dimer and O<sub>2</sub>, only slightly less than the 23.2 kcal/mol obtained for the triplet peroxide state. This means that the adiabatic excitation energy from the closed shell singlet state of the bis- $\mu$ -oxo structure to the triplet state is 21.4 kcal/mol. The spins on copper for the triplet state are –0.05 and 0.58 and on the oxygens 0.53 and 0.58.

**d. Transition State for O<sub>2</sub> Activation.** By far the most time of the present project was spent locating the transition state for O<sub>2</sub> activation between the peroxide and bis- $\mu$ -oxo structures. Since the ground state of the peroxide is a triplet state (in the computations essentially equivalent to an antiferromagnetically coupled singlet state, see above) and the ground state of the bis- $\mu$ -oxo structure is a singlet, there are three different possible types of O–O activation. The first one is an activation on the triplet surface, the second is an activation on the singlet surface, and the third one is an activation by means of a crossing between the singlet and triplet surfaces at an intermediate O–O distance. It is our general experience that bond activations seldom occur according to the third alternative, and this is not the case here either. For the first alternative with a bond activation on the triplet surface, the surface crossing should occur for the product, probably close to the product equilibrium. For the second alternative with a crossing on the singlet surface, the surface crossing should instead occur for the reactant. Since for the reactant, the adiabatic excitation energy to the singlet is 14.8 kcal/mol, the barrier following this mechanism should be at least as high, probably substantially higher. Since no promotion is needed for the triplet state, a dissociation on this surface appears much more likely, and this is also found to be the case.

A major problem in finding the transition state for O<sub>2</sub> activation is that the O–O distance is not the only important

internal reaction coordinate. There is strong coupling between the O–O distance to the Cu–O distances, the Cu–O<sub>2</sub>–Cu bending and also to some Cu–N distances. Several attempts had to be interrupted because one additional formimine ligand started to depart. Also, starting the transition state search using shorter O–O distances than the finally optimized transition state distance did not work either. The search had to be started using substantially longer O–O distances. After many attempts, a transition state was located which smoothly goes from the reactant triplet peroxide in Figure 4 to the product triplet state in Figure 5 with only one long Cu–N distance at any point. This transition state is shown in Figure 6. The Hessian of this structure was too expensive to calculate at the present level of optimization, but at the Hartree–Fock level there is one clearly dominating imaginary frequency of O–O character.

The O–O distance of 1.91 Å for the transition state structure in Figure 6 is close to the average of the triplet reactant and product O–O distances of 1.54 and 2.32 Å, respectively. The structure shows significant bending with an Cu–O<sub>2</sub>–Cu angle of 122° much closer to the reactant angle of 116° than the product angle of 180° (no bending). The spins on the copper atoms are 0.21 and 0.47, and on the oxygen atoms 0.33 and 0.34, compared to 0.49 and 0.53 for copper and 0.21 and 0.16 for oxygen for the reactants. There is thus some asymmetric distortion of the wave function at the transition state and the spins also increase somewhat on the oxygens, as expected when the O–O bond is being broken. The Cu–N ligand distances are quite constant from reactants to products with one long Cu–N distance. The problems encountered in the optimization of the transition state of departing ligands do thus not lead to any substantial changes of the Cu–N distances for the optimized structures finally obtained. The barrier height for the O–O bond breaking is 15.1 kcal/mol, corresponding to a rate on the order of 10<sup>2</sup> s<sup>–1</sup>, which is quite close to the experimental rate of 10<sup>3</sup> s<sup>–1</sup>.<sup>1</sup> This agreement is in fact surprisingly good, both since the rate depends exponentially on the barrier height and also considering the model character of the present study. The barrier obtained using ammonia ligands is 13.6 kcal/mol, quite close to the value obtained for formimine ligands. This similarity shows the stability of the results with respect to the model used, and also gives some confidence in the use of the ammonia ligands for the subsequent steps of the tyrosinase reaction sequence.

**e. Phenol Oxidation of the Tyrosinase Reaction Sequence.** The phenol oxidation part of the pathway was modeled with vinyl alcohol as substrate. In the present work, which we regard only as a preliminary study of the phenol oxidation, only a radical pathway was investigated that does indeed lead to the correct products and we report this here. The reason this pathway was chosen is that this is the simplest approach to test computationally. A study of the electrophilic mechanism, which appears to be the most plausible mechanism based on experimental evidence, will be presented in a future paper.

The relative energies for the entire tyrosinase reaction sequence using ammonia ligands are given in Table 2 and Figure 7. The first part of this reaction sequence has already been discussed above but a few comments should be added. As seen in a comparison of Figures 4 and 7, there are some differences between the results for the two sets of ligands. The major part of this discrepancy comes from the results for the Cu(I) monomer, which represents the zero-energy reference. For this system, the formimine ligands give a structure quite similar to the one using the imidazole ligands, which is close to the X-ray structure. As discussed above, with the ammonia ligands that lack  $\pi$ -bonding ability, one of the ligands departs from the metal

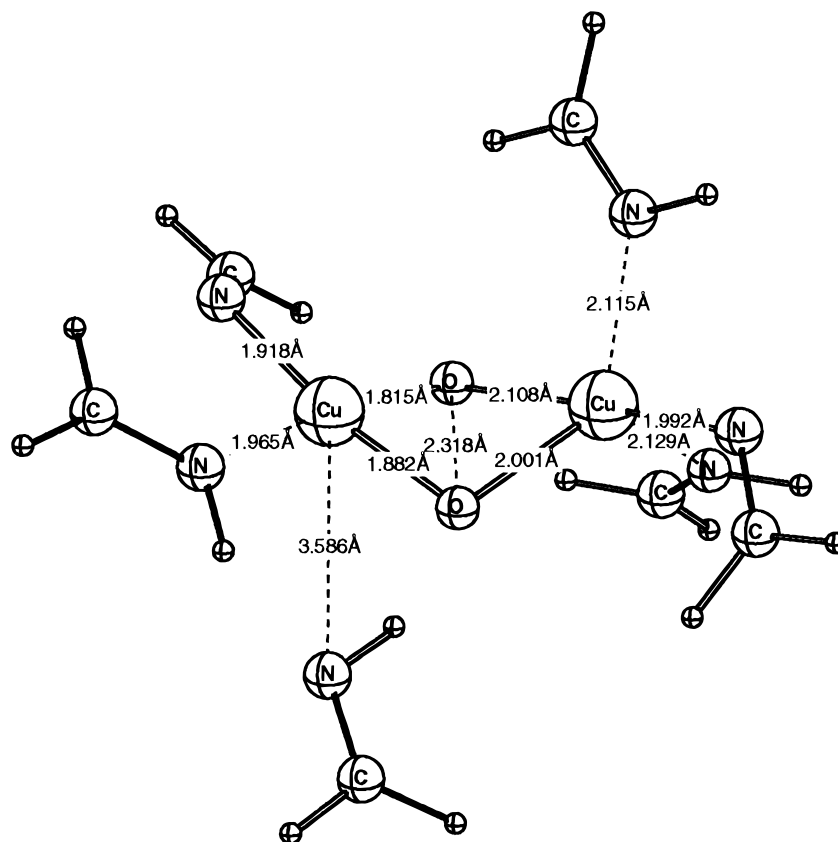


**Figure 5.** Optimized geometry for the triplet bis- $\mu$ -oxo structure.

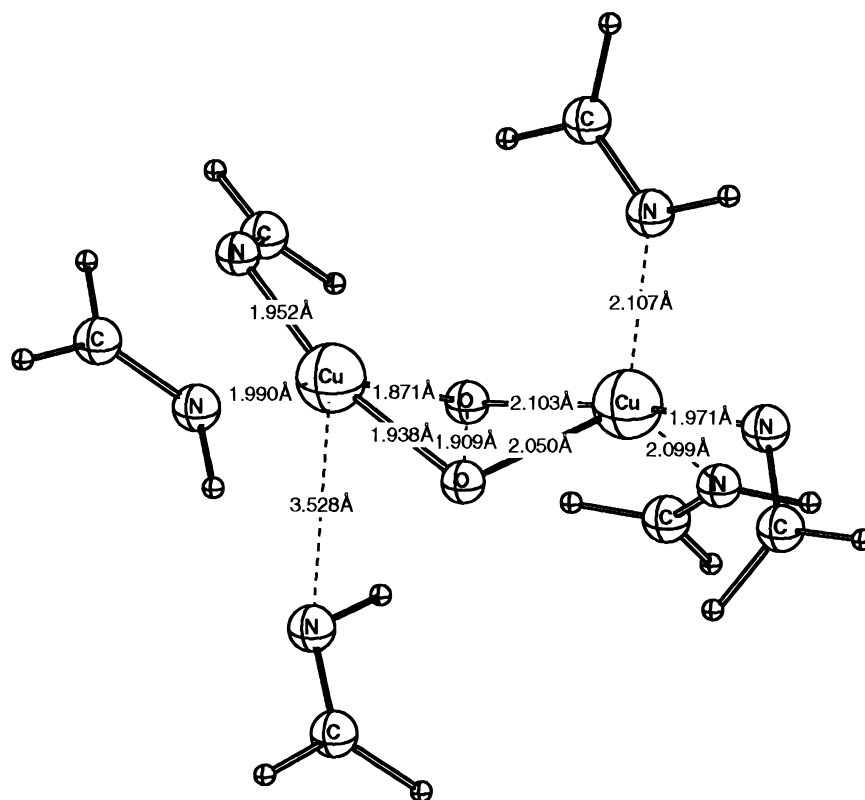


**Figure 6.** Optimized geometry for the triplet transition state for  $O_2$  activation.

and forms quite strong second sphere hydrogen bonds, which leads to an artificial lowering of each monomer by about 5 kcal/mol. Apart from this effect, which affects the relative energy with respect to the monomers, all other relative energies are essentially equal between the two ligand sets. As already noted

above, the barrier is quite similar, and the relative energy between the triplet peroxide and the singlet bis- $\mu$ -oxo structure is 20.6 kcal/mol for the ammonia ligands and 15.4 kcal/mol for the formimine ligands. For this reason the remaining steps of the reaction sequence were only studied using ammonia

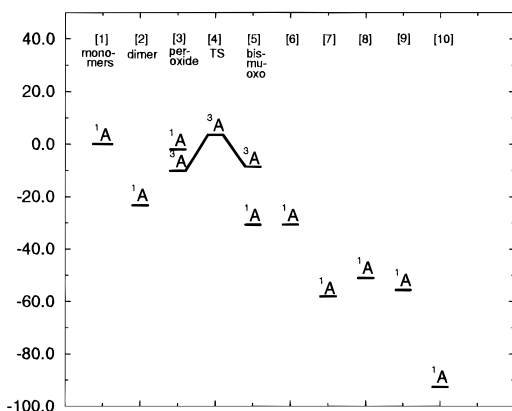


**Figure 7.** Energy diagram for the entire reaction sequence using ammonia ligands.

ligands. No barriers were determined but only the relative energies of the stable intermediates for the remaining steps.

The first step after the  $O_2$  bond has been activated is suggested to be a hydrogen atom abstraction from tyrosine, here modeled by vinyl alcohol, see Scheme 1. This step is found to be almost perfectly thermoneutral (0.1 kcal/mol endothermic) and is expected to occur easily. Hydrogen atom transfers between  $O-H$  bonds have been found both experimentally<sup>29</sup> and theoretically<sup>30</sup> to have low activation barriers. In the resulting geometry of the dicopper complex, the  $Cu-O$  distances become only slightly distorted from those in the singlet bis- $\mu$ -oxo complex, which means that the distances to the  $\mu$ -oxo and the hydroxyl groups are quite similar. The spin distribution in the product has 0.44 and 0.42 spins on copper and  $-0.10$  and  $0.01$  (OH) spins on oxygen.

In the next step, the bridging hydroxyl group is abstracted by the vinyloxy radical to form a glycolaldehyde molecule in a rebound step similar to the one proposed in P-450 oxidations of  $C-H$  bonds. This molecule actually prefers to hydrogen bond to the ligands rather than to form a bridge bond between the coppers in the product. The reaction is substantially exothermic by 27.5 kcal/mol and should occur very easily, probably almost without any barrier.

The next step is an enolization of the glycolaldehyde to a enediol system, which is slightly endothermic by 7.2 kcal/mol. The product forms hydrogen bonds to the ligands, such as the reactant does, and this effect does therefore not contribute much to the reaction energy. Without the copper complex, the energy difference between the glycolaldehyde and the enediol is 8.8 kcal/mol. The endothermicity of this step, in particular combined with a possible barrier, might lead to a problem for the radical mechanism suggested here, and could be a reason another mechanism is preferred in reality.

In the next step a hydrogen atom is abstracted by the remaining bridging  $\mu$ -oxo ligand from the dialcohol to create a bridging enediolate. This step is similar to the previous abstraction steps and should also have a low barrier. It is found to be exothermic by 4.7 kcal/mol.

In the final step, the starting copper dimer is regenerated and the final product glyoxal is formed. This is a quite exothermic process (by 37.0 kcal/mol) and should again occur very easily. This completes the reaction cycle and conforms with the experimental result that it is the  $O_2$  activation step that is rate determining.

**f. Comparison with Prior Mechanistic Work.** Some of the steps of Scheme 1, particularly those involved in  $O_2$  activation, have been proposed in similar form in prior work.<sup>1,11</sup> The phenol oxidation sequence, involving radical intermediates rather than

electrophilic attack, differs from the prior proposals, however. As already mentioned, the electrophilic mechanism will be addressed in future work. Our work does suggest that the possibility of a radical mechanism for substrate oxidation needs to be considered. Mechanistic tests for such a mechanism in the enzyme might therefore be worthwhile, although any radical intermediates are likely to have very short lifetimes, being constrained in the active site. A notable feature of Figures 4-6 is the presence of three firmly bound N-ligands on one copper, but of only two on the other. The third N-ligand originally bound to  $Cu-A$  has retreated to more than 3.5 Å, a clearly nonbonding distance. The same trend is seen in the long axial  $Cu-N$ (His) distances found in the crystal structure of oxy-hemocyanin, although the axial His does not undergo complete decomplexation, as in the quantum chemical model. The difference is most probably due to the  $N-H\cdots O$  hydrogen bonding to the bridging O, possible in the model but not in the real His ligand. While a strongly bound formimine would probably not be affected by the possibility of H-bonding, a weakly bound one, such as the axial ligand in a  $Cu(II)$  square pyramid, should be much more easily induced to dissociate fully in this way. The EPR signal for inhibited half met tyrosinase is most consistent<sup>1</sup> with a distorted trigonal bipyramidal geometry at  $Cu(II)$ . In line with this suggestion, the structures of the 5-coordinate  $Cu$  site in most of the intermediates studied is indeed best described as trigonal bipyramidal. An issue in prior work<sup>1</sup> has been whether the  $O-O$  bond cleaves before, with or after phenol coordination. The present proposed cycle has  $O-O$  cleavage preceding phenol coordination. Our proposal is consistent with the important functional modeling work of Karlin<sup>8</sup> to the extent that a noncoordinated arene ring is hydroxylated in that work by an adjacent dicopper(I) site in the presence of dioxygen. Mechanistic work on the model system shows that the arene oxidation certainly goes via an electrophilic mechanism, however,<sup>1,11</sup> not via the radical pathway which is the only one we report here.

#### IV. Conclusions

In the present quantum chemical studies (DFT-B3LYP) on a neutral model tyrosinase system,  $L_3Cu\cdots CuL_3$ , the work has been concentrated on the early stages of the tyrosinase reaction sequence. Only one possible pathway, dictated mainly by computational simplicity, has been investigated for the later steps. The first set of calculations were performed for the reacting dimer, which turned out to be more difficult to model than expected. Using ammonia ligands a surprisingly strong bond of 23.2 kcal/mol between the two  $Cu(I)L_3$  monomers was formed. Inspection of the resulting dimer structure indicated that this bonding was largely due to strong bridging hydrogen bonds, which cannot form between the real histidine ligands. Using formimine ligands instead of ammonia gave the same result with a binding energy of 22.5 kcal/mol, even though these ligands have fewer possibilities to form the artificial hydrogen bonds. At this stage there was no choice but to choose the more realistic but expensive imidazole ligands. This calculation led to departure of the monomers and thus confirmed the previous expectation that the high binding energy between the monomers with the simpler ligand models was artificial.

The tyrosinase reactions start by the formation of a  $\mu-\eta^2-\eta^2$  peroxo  $Cu(II)-Cu(II)$  bridging peroxide complex between the reacting copper dimer and  $O_2$ . The calculations show that this is an antiferromagnetically coupled singlet complex. However, a ferromagnetically coupled triplet state, which is much easier to treat computationally, gave both a structure and an energy that are very similar to the antiferromagnetic case, so this type

of coupling was used in the following step. This step is the breaking of the O—O bond which turns out to occur on the peroxide surface, leading to a bis- $\mu$ -oxo product where the O—O bond is entirely broken. This product is in an excited state and will exothermically convert to the closed shell singlet Cu(III)—Cu(III) bis- $\mu$ -oxo ground state only after the dissociation is completed. The computed barrier using formimine ligands is 15.1 kcal/mol and using ammonia ligands it is 13.6 kcal/mol, leading to a rate of dissociation that is consistent with the observed rate of  $10^3 \text{ s}^{-1}$  for the overall tyrosinase reaction sequence. This result is also consistent with a previous assumption that O—O bond breaking is rate limiting. The mechanism for the dissociation is entirely in accord with prior mechanistic suggestions.<sup>1,10,11</sup>

In a very preliminary study of possible subsequent steps, a possible radical pathway was investigated. This pathway starts with a hydrogen abstraction from the OH group of the model substrate, vinyl alcohol, leading to a vinyloxy radical that traps the bridging OH group of the cluster by a "rebound" mechanism. Tautomerization of the resulting bound glycolaldehyde to bound ethenediol is followed by H atom transfer to the other  $\mu$ -oxo group to complete the sequence. The calculations show that this radical pathway at least can be regarded at this stage as a plausible alternative to the previously proposed electrophilic pathway.

## References and Notes

- (1) Solomon, E. I.; Sundaram, U. M.; Machonkin, T. E. *Chem. Rev.* **1996**, *96*, 2563; Kitajima, M.; Moro-Oka, Y. *Chem. Rev.* **1994**, *94*, 737.
- (2) Lerch, K. In *Encyclopedia of Inorganic Chemistry*, King, R. B., Ed.; Wiley: Chichester, 1994, p 850.
- (3) Volbeda, A.; Hol, W. G. *J. Mol. Biol.* **1989**, *209*, 249.
- (4) Magnus, K. A.; Hazes, B.; Ton-That, H.; Bonaventura, C.; Bonaventura, J.; Hol, W. G. *J. Proteins* **1994**, *19*, 302.
- (5) van Gelder, C. W. G.; Flurkey, W. H.; Wichers, H. J. *Phytochemistry* **1997**, *45*, 1309.
- (6) Solomon, E. I. In *Copper Proteins*; Spiro, T. G., Ed.; Wiley: NY 1981; Vol. 3, p 41. Kitajima, N.; Fujisawa, K.; Fujimoto, C.; Moro-Oka, Y.; Hashimoto, S.; Kitagawa, T.; Toriumi, K.; Tatsumi, K.; Nakamura, K. *J. Am. Chem. Soc.* **1992**, *114*, 1277.
- (7) Kitajima, N. In *Encyclopedia of Inorganic Chemistry*; King, R. B., Ed.; Wiley: Chichester, 1994; p 822.
- (8) Tyeklar, Z.; Karlin, K. D. *Acc. Chem. Res.* **1989**, *22*, 241. Karlin, K. D.; Hayes, J. C.; Gultneh, Y.; Cruse, R. W.; McKown, J. W.; Hutchison, J. P.; Zubieta, J. *J. Am. Chem. Soc.* **1984**, *106*, 2121. Nasir, M. S.; Cohen, B. I.; Karlin, K. D. *J. Am. Chem. Soc.* **1992**, *114*, 2482.
- (9) Cooksey, C. J.; Garratt, P. J.; Land, E. J.; Pavel, S.; Ramsden, C. A.; Riley, P. A.; Smit, N. *J. Biol. Chem.* **1997**, *272*, 26226. Clews, J.; Cooksey, C. J.; Garratt, P. J.; Land, E. J.; Ramsden, C. A.; Riley, P. A. *J. Chem. Soc., Chem. Commun.* **1998**, 77.
- (10) Halfen, J. A.; Mahapatra, S.; Wilkinson, E. C.; Kaderli, S.; Que, L.; Tolman, W. B. *Science* **1996**, *271*, 1397.
- (11) (a) Wilcox, D. E.; Porras, A. G.; Hwang, Y. T.; Lerch, K.; Winkler, M. E.; Solomon, E. I. *J. Am. Chem. Soc.* **1985**, *107*, 4015. Solomon, E. I.; Lowery, M. D. *Science* **1993**, *259*, 1575. (b) Sanchez-Ferrer, A.; Rodriguez-Lopez, J. N.; Garcia-Canovas, F.; Garcia-Carmona, F. *Biochim. Biophys. Acta* **1247**, 1995, 1.
- (12) Bernardi, F.; Bottoni, A.; Casadio, R.; Fariselli, P.; Rigo, A. *Int. J. Quantum Chem.* **1996**, *58*, 109–119.
- (13) Bernardi, F.; Bottoni, A.; Casadio, R.; Fariselli, P.; Rigo, A. *Inorg. Chem.* **1996**, *35*, 5207–5212.
- (14) Becke, A. D. *Phys. Rev.* **1988**, *A38*, 3098. Becke, A. D. *J. Chem. Phys.* **1993**, *98*, 1372. Becke, A. D. *J. Chem. Phys.* **1993**, *98*, 5648.
- (15) Frisch, M. J.; Trucks, G. W.; Schlegel, H. B.; Gill, P. M. W.; Johnson, B. G.; Robb, M. A.; Cheeseman, J. R.; Keith, T.; Petersson, G. A.; Montgomery, J. A.; Raghavachari, K.; Al-Laham, M. A.; Zakrzewski, V. G.; Ortiz, J. V.; Foresman, J. B.; Cioslowski, J.; Stefanov, B. B.; Nanayakkara, A.; Challacombe, M.; Peng, C. Y.; Ayala, P. Y.; Chen, W.; Wong, M. W.; Andres, J. L.; Replogle, E. S.; Gomperts, R.; Martin, R. L.; Fox, D. J.; Binkley, J. S.; Defrees, D. J.; Baker, J.; Stewart, J. P.; Head-Gordon, M.; Gonzalez, C.; Pople, J. A. *Gaussian 94*, Revision B.2; Gaussian, Inc.: Pittsburgh, PA, 1995.
- (16) Stevens, P. J.; Devlin, F. J.; Chabrowski, C. F.; Frisch, M. J. *J. Phys. Chem.* **1994**, *98*, 11623.
- (17) Lee, C.; Yang, W.; Parr, R. G. *Phys. Rev.* **1988**, *B37*, 785.
- (18) Vosko, S. H.; Wilk, L.; Nusair, M. *Can. J. Phys.* **1980**, *58*, 1200.
- (19) Perdew, J. P.; Wang, Y. *Phys. Rev. B* **1992**, *45*, 13244. Perdew, J. P. In *Electronic Structure of Solids*; Ziesche, P., Eischrig, H., Eds.; Akademie Verlag: Berlin, 1991. Perdew, J. P.; Chevary, J. A.; Vosko, S. H.; Jackson, K. A.; Pederson, M. R.; Singh, D. J.; Fiolhais, C. *Phys. Rev. B* **1992**, *46*, 6671.
- (20) Hay, P. J.; Wadt, W. R. *J. Chem. Phys.* **1985**, *82*, 299.
- (21) Pavlov, M.; Siegbahn, P. E. M.; Blomberg, M. R. A.; Crabtree, R. H. *J. Am. Chem. Soc.* **1998**, *120*, 548–555.
- (22) Siegbahn, P. E. M.; Svensson, M.; Westerberg, J.; Crabtree, R. H. *J. Phys. Chem.* **1998**, *B102*, 1615–1623.
- (23) Mahapatra, S.; Halfen, J. A.; Wilkinson, E. C.; Pan, G.; Wang, X.; Young, V. G., Jr.; Cramer, C. J.; Que, L., Jr.; Tolman, W. B. *J. Am. Chem. Soc.* **1996**, *118*, 11555.
- (24) Hazes, B.; Magnus, K. A.; Bonaventura, C.; Bonaventura, J.; Dauter, Z.; Kalk, K. H.; Hol, W. G. *J. Protein Sci.* **1993**, *2*, 597.
- (25) Lerch, K. *Metal Ions in Biological Systems*; Sigel, H., Ed.; M. Dekker: NY; 1981; Vol. 3, Chapter 5.
- (26) Siegbahn, P. E. M.; Crabtree, R. H. *J. Am. Chem. Soc.* **1997**, *119*, 3103.
- (27) Blomberg, M. R. A.; Siegbahn, P. E. M.; Styring, S.; Babcock, G. T.; Åkermark, B.; Korall, P. *J. Am. Chem. Soc.* **1997**, *119*, 8285.
- (28) Ryde, U.; Olsson, M. H. M.; Pierloot, K.; Roos, B. O. *J. Mol. Biol.* **1996**, *261*, 586–596.
- (29) Mahoney, L. R.; DaRooge, M. A. *J. Am. Chem. Soc.* **1975**, *97*, 4722–4731.
- (30) Siegbahn, P. E. M.; Blomberg, M. R. A.; Crabtree, R. H. *Theor. Chem. Acc.* **1997**, *97*, 289.